Available online at www.sciencedirect.com
SCIENCE DIRECT®

International Journal of Machine Tools & Manufacture 43 (2003) 1579–1593

INTERNATIONAL JOURNAL OF MACHINE TOOLS & MANUFACTURE DESIGN, RESEARCH AND APPLICATION

On the mechanics of the grinding process – Part I. Stochastic nature of the grinding process

Zhen Bing Hou, Ranga Komanduri *

School of Mechanical and Aerospace Engineering, Oklahoma State University, 218 Engineering North, Stillwater, OK 74078 5016, USA

Received 4 April 2003; accepted 2 July 2003

Abstract

Grinding of metals is a complex material removal operation involving cutting, ploughing, and rubbing depending on the extent of interaction between the abrasive grains and the workmaterial under the conditions of grinding. It is also a stochastic process in that a large number of abrasive grains of unknown geometry, whose geometry varies with time, participate in the process and remove material from the workpiece. Also, the number of grains passing through the grinding zone per unit time is extremely large. To address such a complex problem, it is necessary to analyze the mechanics of the grinding process using probability statistics, which is the subject of this investigation. Such an analysis is applicable to both form and finish grinding (FFG), such as surface grinding and stock removal grinding (SRG), such as cut-off operation. In this investigation, various parameters of the process including the number of abrasive grains in actual contact, the number of actual cutting grains per unit area for a given depth of wheel indentation, the minimum diameter of the contacting and cutting grains, and the volume of the chip removed per unit time were determined analytically and compared with the experimental results reported in the literature. Such an analysis enables the use of actual number of contacting and cutting grains in the grinding wheel for thermal and wheel wear analyses. It can also enable comparison of analytical work with the experimental results and contribute towards a better understanding of the grinding process. The analysis is applied to some typical cases of fine grinding and cut-off operations reported in the literature. It is found that out of a large number of grains on the surface of the wheel passing over the workpiece per second (~million or more per second), only a very small fraction of the grains merely rub or plough into the workmaterial (~3.8% for FFG and ~18% for SRG) and even a smaller fraction (~0.14% for FFG and ~1.8% for SRG) of that participate in actual cutting, thus validating Hahn's rubbing grain hypothesis.

Keywords: Form and finish grinding (FFG); Stock removal grinding (SRG); Cut-off operation; Fine grinding; Abrasives; Grinding wheels

1. Introduction

Grinding, in general, is a very complex material removal operation involving cutting as well as plowing and rubbing between the abrasive grains and the workmaterial [1,2]. Shaw [1] classified the grinding process into two categories, namely, form and finish grinding (FFG) and stock removal grinding (SRG). The primary objective in FFG is to obtain the required form, finish, and accuracy while the primary objective in SRG is to obtain high removal rate. In FFG, fine grain size (generally >100) conventional abrasives (e.g. alumina, SiC) in a vitrified bonded grinding wheel are generally used. The wheels are periodically dressed, conditioned, and trued to maintain sharp cutting edges, to remove metal build-up on the grains or loading of the wheel (metallic chips occupying in the void space between the grains), and to maintain roundness of the wheel. In SRG, coarse grain size (~24–46) abrasives, such as regular alumina, alumina–zirconia are used in a resin bonded grinding wheel. Sometimes, the cut-off wheels are reinforced with fiberglass to prevent catastrophic failure during use. Cut-off and snagging operations come under the category of SRG. Abrasive cut-off is used for parting materials and snagging is used for cleaning of the castings (namely, removal of gates, runners, risers from castings). The wheels used in the cut-off operation are consumed without ever being dressed.

* Corresponding author. Tel.: +1-405-744-5900; fax: +1-405-744-7873.
E-mail address: ranga@ceat.okstate.edu (R. Komanduri).

0890-6955/$ - see front matter
doi:10.1016/S0890-6955(03)00186-X

Nomenclature

A_x	cross-sectional area of chip (mm^2)
a_0	down feed in fine grinding (mm)
b	width of cut (mm)
d or d_{mean}	mean diameter of grains for a standard grain size (mm)
d_{max}	diameter of the largest grain for a standard grain size (mm)
d_{min}	diameter of the smallest grain for a standard grain size (mm)
$d_{cont.min}$	diameter of the smallest actual contacting grain (mm)
$d_{cut.min}$	diameter of the smallest actual cutting grain (mm)
f	down feed in the cut-off operation (mm/s)
g	standard grain size, non-dimensional integer
ℓ	length of cut (mm)
N_ℓ	number of grains per unit length (grains/cm)
N_a	number of grains per unit area (grains/cm^2)
N_v	number of grains per unit volume (grains/cm^3)
$N_{a.cont}$	number of actual contacting grains per unit area (grains/cm^2)
$N_{a.cut}$	number of actual cutting grains per unit area (grains/cm^2)
N_{total}	total number of grains passing through grinding area per second (grains/s)
$N_{total.cont}$	total number of actual contacting grains passing through the grinding area per second (grains/s)
$N_{total.cut}$	total number of actual cutting grains passing through the grinding area per second (grains/s)
$P(p)$	complementary probability function (a non-dimensional number)
p	argument of the complementary probability function (non-dimensional number)
r_x	average radius of a grain (mm)
r_a	radius of cutting edge (mm)
r_o	radius of contacting area (mm)
v_{wheel}	peripheral velocity of grinding wheel (m/s)
v_{table}	table speed (mm/s)
V_{chip}	volume of chips (mm^3)
V	total removal rate (mm^3/s)
$V_{rmv.exp}$	total removal rate experimentally measured (mm^3/s)
$V_{rmv.anl}$	total removal rate analytically calculated (mm^3/s)
δ	range of distribution of sizes of grains (mm) $\delta = d_{max} - d_{min}$
Δ_{gx}	depth of grain indentation (mm)
Δ_{ind}	depth of wheel indentation into the work (mm)
$\Phi(p)$	probability function, a non-dimensional number

While both finish grinding and cut-off operations come under the same category of grinding, there are several differences between them. In the cut-off operation, the wheel speed is generally 2–5 times higher than in conventional finish grinding. In the surface grinding, the workpiece reciprocates at a given depth of cut while in the cut-off operation the wheel is fed continuously into the workpiece at a given feed rate. The chip thickness as well as the length of contact (or length of chip) are generally an order of magnitude larger in the cut-off operation than in fine grinding. Consequently, the removal rate is significantly higher in the cut-off operation. Also, the cut-off operation is generally conducted dry (or in air) as water tends to deteriorate the resin and reduce the life of the cut-off wheel, whereas a coolant is invariably used in finish grinding to dissipate the heat generated and to protect the workpiece from "grinding burn." In FFG and SRG operations, both attritious wear and microchipping wear of the abrasive grains take place. However, in the cut-off operation, additional wear occurs due to dislodgment of the whole abrasive grains from the wheel as a result of (a) thermal softening of the resin binder and/or (b) mechanical erosion of the resin binder by the flowing chip, and (c) mechanical removal of bond material due to the pressure developed in the voids by the chips due to insufficient volume. In modeling these processes, these and other issues that affect the performance of the grinding wheel have to be considered carefully.

2. Brief review of literature on FFG and SRG

The mechanics of the grinding process (both FFG and SRG) was investigated extensively by many researchers.

Pioneering work on this topic commenced in the early 1950s at MIT by Prof. Milton Shaw and his associates. For example, Marshall and Shaw [3] investigated the variation of grinding forces in dry surface grinding under different grinding conditions. Backer et al. [4] investigated the so-called *size effect* in metal cutting. They determined the number of contacting grains per unit area for the first time using a carbon-black (soot) replica technique on a glass slide. They offered an explanation for the increase in the specific energy with decreasing chip thickness on the basis of size effect (decrease in the number of defects with decrease in the volume considered). It is now widely accepted that there are other explanations for this difference, including the fact that most abrasive grains present on average a large negative rake angle and there is considerable rubbing between the abrasive grains and the workpiece due to attritious wear of the abrasive grains. Outwater and Shaw [5] investigated the surface temperatures generated in fine grinding and reported temperatures as high as 1163 °C (2125 °F) based on both experimental and analytical work. Reichenbach et al. [6] investigated the role of chip thickness in grinding, while Mayer and Shaw [7] investigated the temperature in grinding experimentally. This work initiated a flurry of research activities in grinding since then. Subsequently, Baker and Merchant [8] investigated the basic mechanics of grinding.

Most researchers considered the grinding process akin to milling process but on a microscale. They considered the cutting and thrust forces to be solely due to cutting and neglected the frictional rubbing forces on the clearance face of the grains. To account for the apparent anomalies between conventional machining and grinding, Hahn [9–11] introduced the rubbing grain hypothesis wherein rubbing forces on the clearance face of the abrasive grain play a major role compared to the forces due to cutting. Part of the justification for this is based on the ratio of tangential to normal forces in grinding. In grinding, this is typically in the range of 0.3–0.5, which is characteristic of a sliding friction process. Subsequently, Komanduri [12] reported an experimental investigation to simulate grinding using high negative rake angles in conventional cutting and showed the similarities between grinding and machining with high negative rake tools. In fact, the large negative rake angles presented by the abrasive grains in grinding can produce this ratio. So, it is not actually necessary to replace cutting altogether with rubbing. However, such an analysis is far simpler to analyze than the combination of cutting and rubbing as the number of cutting grains are only a small fraction of the contacting or rubbing grains.

In this investigation, Hahn's [9–11] approach is used in the analysis of the grinding process. It will be shown that based on statistical analysis of the abrasive grains on the grinding wheel surface in both FFG and SRG, not all grains participate in the cutting action; instead a majority of the grains merely rub due to insufficient depth of cut imposed on these individual grains and even smaller number of grains participate in the actual cutting process. Other major contributors on the mechanics of fine grinding include Malkin [13], Rowe and Wetton [14], Opitz et al. [15], Snoeys et al. [16], Nakayama [17], Rowe et al. [18], Lavine [19], Guo and Malkin [20], Ju et al. [21], to name some. In 1972, an International Grinding Conference [22] was held at Carnegie-Mellon University in Pittsburgh where leaders across the world in this field participated. The proceedings of this conference is a good source of reference material in grinding, for both FFG and SRG. There are similar proceedings, such as the Annals of CIRP, which is also a good source of reference material on the mechanics of grinding.

In the SRG area, especially in the cut-off operation, much of the research work was conducted in the late 1960s at Carnegie-Mellon University (CMU) under the direction of Prof. Shaw and supported by the Grinding Wheel Institute and the Abrasive Grain Association. Shaw et al. [23] investigated the mechanics of the abrasive cut-off operation in considerable detail. As part of that group, Eshghy [24,25] investigated the thermal aspects of abrasive cut-off operation. Shaw [26] also reported a method of rating cut-off wheels based not on conventional parameters, such as the grain size, grade (hardness), and structure number but on the basis of effective number of cutting points per unit area on the wheel, the void space between successive grains, the chip flexibility parameter, and the down-feed rate corresponding to a grinding ratio of unity. These studies at CMU have enabled the determination of the optimum cut-off grinding conditions, improvement of the efficiency of the operation, increase in the life of the cut-off wheel, and improvement of the surface integrity of the workpiece used.

The review presented above is of necessity brief covering only the historical highlights of the process due to space constraints. For a more complete coverage of the literature, references cited in the textbooks by Shaw [1] and Malkin [13] as well as several review articles in the literature may be consulted. Since, material removal in the grinding process involves cutting, plowing, and sliding, it is necessary to determine the contributions of actual cutting versus the other processes on a statistical basis. For that, it is necessary to determine the number of abrasive grains in actual contact per unit area on the wheel, the number of actual cutting grains per unit area, minimum diameter of the contacting and cutting grains, and the average chip volume under different grinding conditions. Since the grinding process is stochastic in nature, in this investigation, the grinding operation is analyzed using the probability statistics. Parts 2 and 3 of this three-part series on the mechanics of grinding deals with the thermal aspects of fine grinding and thermal aspects of SRG, namely, the cut-off operation, respectively. Relevant references on these topics will be covered in those papers.

3. Review on the determination of the number of cutting points

The number of contacting points in a grinding wheel plays an important role both on the mechanics and thermal aspects of grinding. Not all abrasive grains on the surface of a grinding wheel participate in the grinding process. Some may cut, others may rub or plough, and a large number may not be participating in the grinding process at all but to take a free ride. This depends on the grinding wheel specifications (abrasive type and grain size as well as the bond, hardness, and structure of the wheel), the wheel (abrasive)–work material interactions, as well as the grinding conditions (wheel speed, work speed, depth of cut, forces, grinding fluid, etc.) used, and the stiffness and accuracy of the machine tool.

Backer et al. [4] for the first time estimated the number of apparent contact points by rolling the grinding wheel under its own weight on a soot (carbon-black)-covered glass plate. The image is photographically enlarged and projected on to a screen. The number of cutting points per unit area is determined by counting the number of spots. They reported that for a 46-grit alumina wheel, the number of cutting grains per unit area, N_a to be 299 grains/cm^2 (1930 grains/in.^{2}). Backer et al. [4] also pointed out many drawbacks of this technique. It may be noted that this is actually an estimate of the number of peaks on the abrasive grits on the wheel surface that has penetrated the carbon film and not necessarily the number of actual contacting or cutting grains per unit area. It is also not the apparent number of grains per unit area.

For estimating the number of cutting points on a cut-off wheel, Shaw et al. [23] used a technique of rolling the grinding wheel over a piece of Sanborn recording paper and counting the number of contacts. They also used a thin steel band (0.010 in. thick razor blade stock) wrapped around the periphery of the grinding wheel and observed the projected image on to a screen to count the contacting points. All the above techniques are static methods.

Brecker and Shaw [27] developed a dynamic method to determine the effective number of cutting points on the surface of a grinding wheel. It employs a thin workpiece mounted on a special piezoelectric dynamometer of very high natural frequency of response to measure the instantaneous forces. The workpiece is so thin that only one grain is assumed to be in contact at a given time. The number of chips produced in a given time is determined by counting the number of force peaks. While there are some limitations associated with this technique, it is by far the more accurate method for obtaining the number of cutting points under dynamic conditions.

4. Statistical treatment of the grinding operation

The analytical model presented in the present investigation should be considered as somewhat simplistic or as a first approximation in view of the complex nature of the grinding process. Several assumptions listed in the following are made in this analysis: (1) the analysis is based on the statistical distribution (normal) of the abrasive grains of nominal grain size on the grinding wheel surface, (2) while dressing plays an important role in grinding, its effect is not considered in the present analysis, i.e. the grain distribution with and without dressing is assumed the same, (3) local elastic deflections between the wheel and the workpiece depends on several variables, as discussed by Rowe et al. [28]. For example, Rowe et al. [28] reported that the measured contact length varies from 50% to 200% greater than the geometric contact length. This has to be taken into consideration in the analysis of the mechanics of grinding. In this investigation, some consideration is given to the local elastic deflections between the wheel and the workpiece as well as the abrasive grains and the workpiece. The exact effect depends on the wheel–work–machine tool interaction under grinding conditions, (4) most of the grinding energy is attributed to rubbing, following Hahn's rubbing grain hypothesis [9–11], (5) the fine grinding process is considered under dry or no lubricating conditions, and finally, (6) the minimum depth of grain indentation, Δ_{gx} for cutting is taken as $0.05r_x$ where r_x is the average radius of the grain. The critical depth of indentation is then used to determine the number of active cutting grains. Below this depth, only rubbing and/or plowing are considered to take place.

4.1. Determination of the number of contacting grains, active cutting grains, and the chip removal rate

The grain size of an abrasive in a grinding wheel is determined by the number of opening per unit length in the sieve. For example, for the 46-grit, most of the abrasive grains remain on the sieve with 46 openings per linear inch. When determining the grain size, the diameter of the wire mesh used in the sieve should also be taken into account. The wire mesh is of larger diameter for the coarser abrasive sieve and smaller diameter for the finer abrasive sieve. So, in order to determine the size of the abrasive these factors have to be taken into account.

Fig. 1 is a standard marking system for conventional abrasives of different grain sizes [13,29,30]. The coarse grits (grain size from 8 to 24) are mainly used in SRG, the medium grits (grain size 30–60) in semifinish grind-

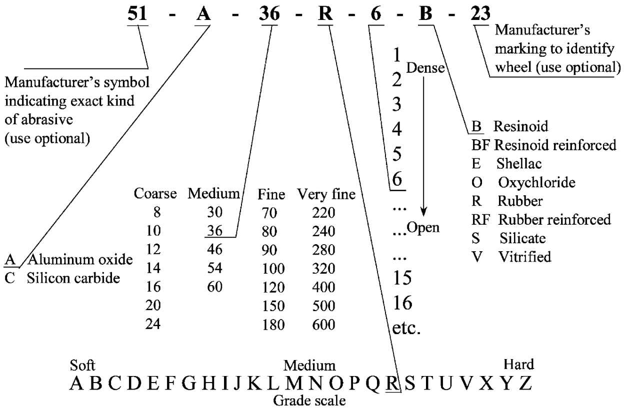

Fig. 1. Standard marking system for grinding wheels using conventional abrasives [13,29,30].

ing, and the fine grits (grain size 70–180) and very fine (grain size 220–600) grits in finish grinding as in FFG.

For the 24-grain size, the maximum diameter is determined using sieve 24 and the minimum diameter using the next finer sieve, namely, 30. For the 46-grit size, the maximum diameter is determined using sieve 46 and the minimum diameter using the next finer sieve, namely, 54. Similarly, for the 100-grit size, the maximum diameter is determined using 100 sieve and the minimum diameter using the next finer sieve, namely, 120.

When the nominal grain size is known, the diameter of the maximum and minimum diameters of the grains can be determined. From this, the mean diameter can be determined as

$$d_{mean} = (d_{max} + d_{min})/2 \quad (1)$$

Table 1 gives values of the sieve openings and the corresponding maximum (d_{max}), minimum (d_{min}), and the mean (d_{mean}) grain diameters for different grain sizes. Fig. 2 is a plot of the mean grain diameter (d in mm) versus the nominal grain size (g) from which the following best-fit equation is obtained

$$d = 28.9g^{-1.18}$$

In the grinding industry, the following empirical relationship is commonly used between the grain size (g) and the mean grain diameter (d) in inch units

$$g \times d = 0.6$$

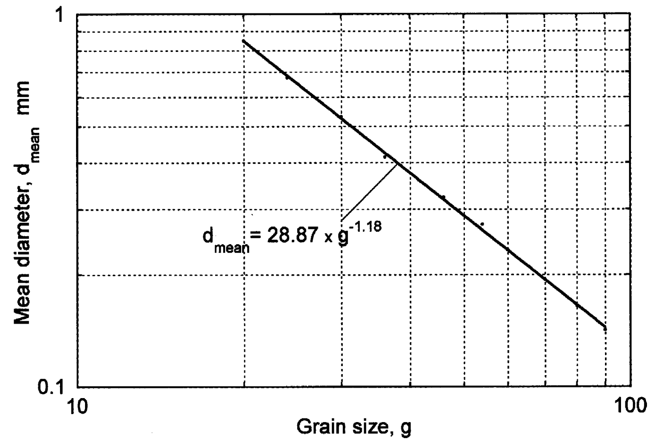

Fig. 2. Plot of the mean grain diameter (d) versus the nominal grain size (g).

For example, a 24-grain size abrasive would have a mean diameter of ~0.025 in. (0.635 mm), a 46-grain size abrasive ~0.013 in. (0.330 mm), and a 100-grain size abrasive ~0.006 in. (0.152 mm). It can be seen that there are some differences in the mean diameter of the grains by these two methods.

The total volume of the wheel comprises of the volume of the abrasive, the binder, and the void space between the grains in the wheel. This depends on the hardness and structure of the wheel used. Tables A1 and B1 in Appendices A and B give approximate percentages of the abrasive, the binder, and the void space for vitrified bonded [31] and resinoid bonded [32] grinding wheels, respectively. The exact formulation may vary slightly from one company to another and is not disclosed for proprietary reasons. For example, it can be seen from Appendix A that for a 32A46H8V conventional vitrified bonded grinding wheel of hardness (H) and structure (8) used in FFG, the abrasive grains occupy ~48%, the bonding material (glass) ~6%, and the void space ~46%, by volume [31]. Similarly, it can be seen from Appendix B that for a A46-R6B or A24-R6B resin bonded cut-off wheel of hardness (R) and structure (6), the abrasive grains occupy ~52%, the bonding material (resin with some fillers) ~30%, and the void space ~18% by volume [32]. Thus even though the volume fraction of the abrasive is about half and not significantly different between a grinding wheel for FFG and a grinding

Table 1
Sizes of sieve openings, d_{max}, d_{min}, and d_{mean}

Grain size #	20	24	30	36	46	54	60	70	80	90	100
Sieve opening (mm)	0.938	0.762	0.589	0.476	0.354	0.291	0.255	0.211	0.178	0.152	0.142
d_{max} (mm)	0.938	0.762	0.589	0.476	0.354	0.291	0.255	0.211	0.178	0.152	0.142
d_{min} (mm)	0.762	0.589	0.476	0.354	0.291	0.255	0.211	0.178	0.152	0.142	0.114
d_{mean} (mm)	0.850	0.676	0.532	0.415	0.323	0.273	0.233	0.194	0.165	0.147	0.128

wheel for cut-off, there is a significant difference between the volume of bonding material and void space between these two types of wheels. For example, in the grinding wheel for FFG, the bonding material is ~6%, and the void space is ~46% by volume while in the cut-off wheel, the bonding material is ~30%, and the void space is ~18% by volume. This will affect the void space between the grains. Since, the abrasives are bonded chemically with the glass binder in the case of vitrified bonded grinding wheel, less binder (~6%) is sufficient to anchor the grains in the wheel. In the resin bonded wheel, since the bonding between the abrasives and the binder is mechanical, more binder is necessary (30% in this case) to anchor the grains in the binder. From the above considerations, the average number of grains per unit length, N_ℓ on the surface of the grinding wheel is given by

$$N_\ell = \frac{10}{d_{\text{mean}}} \times (\text{volume fraction of the abrasives})^{1/3} \quad (2a)$$

The average number of grains per unit area is given by

$$N_a = N_\ell^2 \quad (2b)$$

and the average number of grains per unit volume is given by

$$N_v = N_\ell^3 \quad (2c)$$

Similarly, the total number of grains passing through the grinding area per second is given by

$$N_{\text{total}} = V \times b \times N_a \quad (3)$$

where V is surface speed of the wheel and b is the width of cut in FFG or the kerf width in the case of cut-off operation.

As already pointed out, in this investigation, we have considered the idealized case of the distribution of abrasive grains on a grinding wheel without due consideration of dressing of the wheel in the case of FFG for simplicity. This number may change depending upon the dressing method and dressing conditions used.

4.1.1. Material removal rates

The experimental removal rate for *fine grinding* is given by:

$$V_{\text{rmv.exp}} = \text{downfeed}(a_0) \times \text{width of cut}(b) \times \text{table speed}(v) \quad (4a)$$

The experimental removal rate for *cut-off operation* is given by:

$$V_{\text{rmv.exp}} = \text{length of cut}(\ell) \times \text{width of cut}(b) \times \text{rate of down feed}(f) \quad (4b)$$

4.2. Minimum depth of grain indentation for cutting

In ultraprecision machining with a single crystal diamond tool depending on the geometry of the tool, there appears to be a minimum depth of cut below which chip formation may not occur. This critical depth of cut is reported to be ~$0.05r_a$ (r_a is the edge radius of the cutting tool and the coefficient 0.05 is obtained experimentally). In grinding, the radius of the cutting edge of the abrasive grain is random but its average value is known, namely, the average radius of the grain, r_x (Fig. 3). In this investigation, if the grain indentation Δ_{gx} (depth of cut) is larger than $0.05r_x$, it is assumed that cutting will take place. The critical depth of indentation is then used to determine the number of active cutting grains. Below this depth, only rubbing and/or ploughing are considered to take place. The number of contacting grains undergoing rubbing are determined from this.

4.3. Distribution of the abrasive grains on the grinding wheel surface

In the manufacture of grinding wheels, there is no special measure taken to select only one grain size, namely, the nominal grain size of the abrasive for a given grain size wheel (for example, in a 32A46H8V wheel, the nominal grain size is 46). Instead, the distribution of the grain sizes for any given nominal grain size grinding wheel usually takes the form of normal distribution. Some fines and a small fraction of smaller grain sizes are

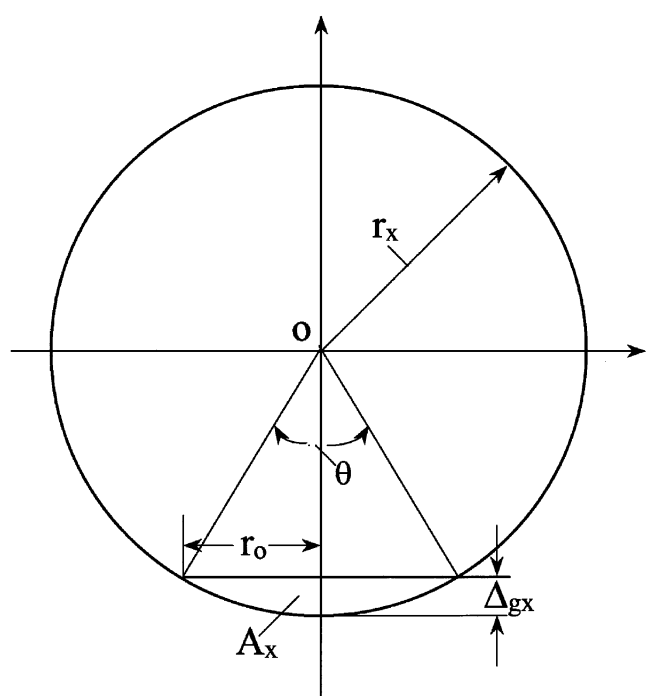

Fig. 3. Schematic showing the relationship between the average radius of a cutting grain (r_x), grain indentation (Δ_{gx}), and chip cross-section (A_x).

intentionally added to the nominal grit size to facilitate consolidation and sintering of the wheel. However, the effect of this is not taken into consideration in the present investigation. Fig. 4(a) is a schematic of the grain size distribution showing (not to scale) the maximum and minimum diameter of the grains and the probability distribution of the other sizes of the grains. Fig. 4(b) shows normal distribution plot of the frequency versus the grain diameter. The most frequent grain size is the mean while the maximum and minimum grain sizes are rarely encountered given by the area towards the tail end on either side of the normal distribution curve. It may be noted that Fig. 4(a) does not show how the grains are distributed on the grinding wheel but merely the size distribution of a given nominal size abrasive in a grinding wheel. Also, the variation in grain size in Fig. 4 is highly exaggerated to illustrate important statistical features. In actual practice this variation is not very significant.The normal distribution is expressed mathematically as

$$y = \frac{1}{\sqrt{2\pi}} e^{-x^2/2} \tag{5}$$

where y is the variation of the frequency with respect to various values of x.

The area under the normal distribution curve, in the range of $-\infty$ to p, is given by the probability density function

$$\Phi(p) = \frac{1}{\sqrt{2\pi}} \int_{-\infty}^{p} e^{-x^2/2} dx \tag{6}$$

The physical interpretation of $\Phi(p)$ is the probability of all the events with various x's in the range of $x = -\infty$ to $x = p$. The results of the numerical integration for various values of the argument p of this special function $\Phi(p)$ can be found in tabular forms in mathematical handbooks [33]. The area $P(p)$ under the normal distribution curve in the range from p to $+\infty$ (complementary of $\Phi(p)$) can be calculated using the tabulated values of $\Phi(p)$ [33] as follows

$$P(p) = 1 - \Phi(p) \tag{7}$$

for

$$\frac{1}{\sqrt{2\pi}} \int_{-\infty}^{+\infty} e^{-x^2/2} dx = 2 \times \frac{1}{\sqrt{2\pi}} \int_{0}^{+\infty} e^{-x^2/2} dx = 2 \times 0.5 = 1$$

Of course, the area $P(p)$ can also be calculated by numerical integration from p to $+\infty$, thus:

$$P(p) = \frac{1}{\sqrt{2\pi}} \int_{p}^{+\infty} e^{-x^2/2} dx \tag{8}$$

In practice, a finite number can be used for the upper limit of integration instead of ∞ with minimal error (refer to Fig. 4) because the normal distribution function converges rapidly and approaches zero for values of $x > 3$. If 3 is considered as the upper limit, the error is ~0.13%. Since the number of grains passing through the grinding zone per second is considerable (~a million or more per second), a higher accuracy is required. In this investigation, a value of 4.4 is considered as the upper limit instead of ∞. Once a definite number is used instead of ∞, the area $P(p)$ under the normal distribution curve in the range of p to that definite number is merely the probability of active grain contacts. The lower limit of p is the argument of the special function $P(p)$, which is the complementary probability function. Here,

$$p = \left(\frac{\delta}{2} - \Delta_{ind}\right) \times \frac{4.4}{\delta/2} \tag{9}$$

and

$$\delta = d_{max} - d_{min} \tag{10}$$

where δ is the range of grain size distribution and Δ_{ind} is the depth of wheel indentation. The data for $\Phi(p)$ available in many mathematical handbooks is given only up to four significant places which is not of sufficient accuracy for grinding application where the number of

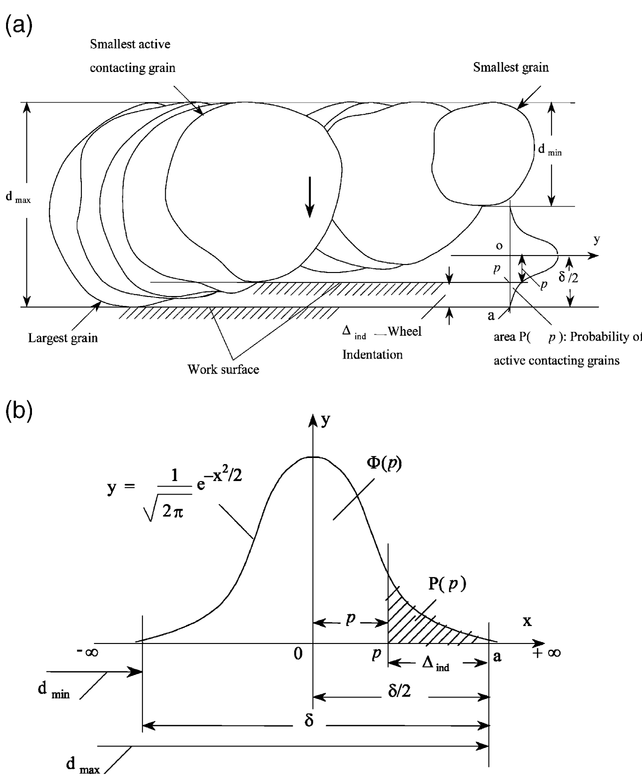

Fig. 4. (a) Schematic of the grain size distribution showing maximum and minimum diameters of the grain and the probability distribution of other sizes of the grains; (b) Normal distribution plot of the frequency versus the grain diameter.

grains passing through the grinding zone per second is considerable (~million grains/s). Hence, the function $P(p)$ was calculated with an accuracy of up to six significant places using direct numerical integration from p to +4.4. Table C1 in Appendix C gives values of $P(p)$ in a tabular form for convenience.

4.4. Determination of the probability of active contacting grains and active cutting grains

Fig. 5 is a schematic showing the relationship between the probability of active contacting grains, active cutting grains, and the indentation of the wheel into the work Δ_{ind}. Let us first investigate the probability of active contacting grains. It can be seen from Fig. 5, the diameter of the smallest contacting grain is given by $d_{cont.min} = d_{max} - \Delta_{ind}$. Grains with diameter larger than $d_{cont.min}$ all contact the work surface at different depths of grain indentation, Δ_g, where Δ_g varies from 0 to Δ_{ind}.

It can be seen that larger the wheel indentation, the more the number of contacting grains and larger the area under the normal distribution curve from p_1 to p_{max}. Hence, larger is the probability of active contacting grains. When Δ_{ind} is known, then

$$x_1 = \delta/2 - \Delta_{ind} = \frac{d_{max} - d_{min}}{2} - \Delta_{ind} \tag{11}$$

Then the equivalent argument p_1 of the special function $P(p)$ (Eq. (8)) can be calculated using the law of proportions, as follows

$$p_1 = x_1 \times \frac{4.4}{\delta/2} \tag{12}$$

The corresponding probability of active contacting grains $P(p_1)$ can be found using Table 1 or by numerical integration of Eq. (8) directly from p_1 to 4.4 (p_{max} = 4.4).

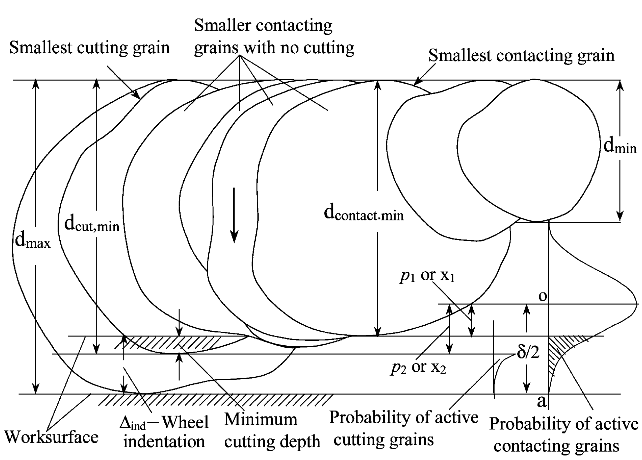

Fig. 5. Schematic showing the relationship between the probability of active contacting grains, active cutting grains and the indentation of the wheel into the workmaterial.

Fig. 5 also shows the relationship between the size of the minimum active cutting grains and minimum active contacting grains. It can be seen that minimum diameter of the cutting grains is given by

$$d_{cut.min} = d_{cont.min} + \text{minimum cutting depth} \tag{13}$$

As discussed in Section 4.2, the minimum cutting depth is taken as $0.05r_a$, where r_a is the radius of the cutting grains of minimum size.

Thus, the minimum diameter of the cutting grains is given by:

$$d_{cut.min} = d_{cont.min} + 0.05 \times d_{cut.min}/2,$$

or,

$$d_{cut.min}(1-0.025) = d_{cont.min}, \tag{14}$$

or

$$d_{cut.min} = d_{cont.min}/0.975$$

From Fig. 5, it can be seen that

$$x_2 = x_1 + \text{minimum cutting depth} = x_1 + 0.025 \times d_{cut.min} = x_1 + (0.025/0.975)d_{cont.min} = x_1 + (1/39)(d_{max} - \Delta_{ind}) \tag{15}$$

The corresponding argument p_2 can be calculated using the simple law of proportions, as follows

$$p_2 = x_2 \times \frac{4.4}{\delta/2} \tag{16}$$

Using Table C1 or by numerical integration of Eq. (8) from p_2 to 4.4, the probability of active cutting grains $P(p_2)$ can be found.

4.5. Local elastic deflections and deflections due to finite machine stiffness

Local elastic deflections and deflections due to finite machine tool stiffness need to be considered in the development of an accurate model of the grinding process. These deflections will reduce the actual depth of cut and consequently, the removal rate. They also affect the thickness as well as the length of cut.

Hahn [9–11] developed a simple model consisting of grinding grits mounted on elastic springs by considering the effect of elastic contact between the grinding wheel and the workpiece. Brown et al. [34] subsequently analyzed local elastic deflections by considering two modes of deflection, namely, elastic deflection of the grain–workpiece (micro) and elastic deflection of the wheel–work contact (macro), using Hertzian contact relations. Krug and Honcia [35] estimated the amount of local wheel deflection in grinding and concluded that it is on the order of 1 μm. In the present investigation this was found to be ~0.75 μm.

Rowe et al. [28] reviewed the literature on the deflections that occur within the grinding contact zone. They reported that the measured contact length varies from 50% to 200% greater than the geometric contact length.

The stiffness of the grinding machine is generally in the range of 25–50 N/μm. Under a load of 30 N, the deflection will be ~0.6–1.2 μm. The total deflection due to combined local elastic deflection and deflection due to finite machine tool stiffness will be ~2 μm. To obtain more accurate values of the removal rate, the wheel depth of cut should be reduced by this amount and the contact length increased accordingly in fine grinding.

4.6. Determination of the metal removal rate

The metal removal rate can be calculated analytically by integrating the volume of chips removed by individual cutting grains. For this purpose, a relationship between the geometrical parameters of the chip and the cutting grains has to be developed. Referring to Fig. 3, if the grain shown is a cutting grain, the indentation of it into the work material Δ_{gx} must be larger than 0.05 $\times\, r_x$. The chip cross-section will have the form A_x as shown in the figure. Thus the volume of the chip is given by $A_x \times \ell$, where ℓ is the length of the chip in FFG or the contact length between the workpiece and the wheel in cut-off. The area A_x can be found from mathematical handbook [33] as follows

$$A_x = \frac{1}{2} r_x^2 (\theta - \sin\theta) \tag{17a}$$

where $\theta = 2\arctan\sqrt{1-m^2}/m$ and $m = 1-\Delta_{gx}/r_x$.

The radius of the contacting interface area r_o is given by

$$r_0 = r_x \sin\frac{\theta}{2} \tag{17b}$$

Referring to Figs. 5 and 6, grains larger than $d_{cut.min}$

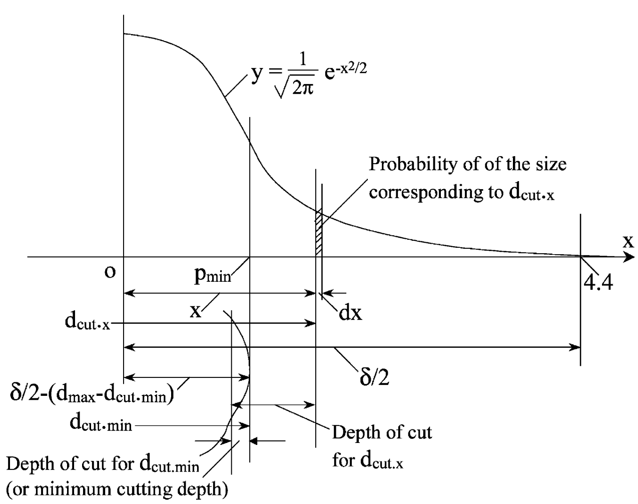

Fig. 6. Probability of the grain size corresponding to $d_{cut.x}$ in the range from $d_{cut.min}$ to d_{max}.

are all active cutting grains. Consider the case of active cutting grains of diameter, $d_{cut.x}$ (see Fig. 6). The shaded area $(1/\sqrt{2\pi})e^{-x^2/2}dx$ is the probability of the grains of diameter $d_{cut.x}$. The depth of cut Δ_{gx} of each of these grains is given by

$$\Delta_{gx} = 0.05 \times \frac{d_{cut.min}}{2} + (d_{cut.x} - d_{cut.min}) \tag{18}$$

For $r_x = d_{cut.x}/2$, the cross-sectional area of the chip A_x generated by a grain of diameter $d_{cut.x}$ can be calculated using Eq. (17a).

The number of cutting grains of diameter

$$d_{cut.x} = N_{total} \times \frac{1}{\sqrt{2\pi}} e^{-x^2/2} dx \tag{19}$$

Volume of the chips removed by the active cutting grains of diameter, $d_{cut.x}$ is given by

$$V_{chip} = A_x \times I \times N_{total} \times \frac{1}{\sqrt{2\pi}} e^{-x^2/2} dx \tag{20}$$

The total removal rate, i.e. due to the contribution of all active cutting grains with diameters from $d_{cut.min}$ to d_{max} is given by

$$V = I \times N_{total} \times \frac{1}{\sqrt{2\pi}} \times \int_{p_{min}}^{4.4} A_x \times e^{-x^2/2} dx \tag{21}$$

where

$$p_{min} = \left[\frac{\delta}{2} - (d_{max} - d_{cut.min})\right] \times \frac{4.4}{\delta/2} \tag{22}$$

(see Fig. 6).

5. Results and discussion

In the following, results of five cases of grinding, namely, one fine grinding and four cut-off operations are considered from the literature [3,23]. Appendix D gives an example calculation for the case of fine grinding in some detail.

The following are the specifications of the grinding wheels and the grinding conditions

1. Example of fine grinding [3]

Grinding wheel: 32A46H8V (alumina abrasive, 46-grit size, vitreous bond, hardness *H*, and structure 8)
Wheel speed, V_{wheel}: 30.48 m/s (6000 fpm)
Table speed, v_{table}: 20.32 mm/s (4 fpm)
Width of cut, b: 12.7 mm (0.5 in.)
Downfeed, a_0: 0.0254 mm (0.001 in.)

.

2. Example of cut-off grinding [23]

Cut-off wheels: A24-R6B and A46-R6B (alumina abrasive, 24 and 46 grit sizes, resin bond, hardness *R* and structure 6)
Wheel speed, V_{wheel}: 63.50 m/s (12,500 fpm)
Down feed rate, *f*: 6.52 mm/s (15.4 ipm)
Width of cut, *b*: 4.76 mm (3/16 in.)
Length of cut, ℓ: 25.4 mm (1 in.) and 50.8 mm (2 in.).

Table 2 summarizes values of various statistical parameters determined using the analysis developed in this paper for one case of fine grinding and four cases of cut-off operation. Let us first compare FFG (Case 1) and SRG (Case 2), namely, the cut-off operation for the same nominal grain size of 46, using Table 1. It can be seen that the length of cut in SRG is an order of magnitude more than in FFG while the wheel speed for this case is ~2 times.

The total number of grains in the grinding wheel passing through the cutting zone per second in both FFG and SRG is ~2 million. The removal rate, however, is ~2 orders of magnitude higher in SRG (773 mm^3/s) than in FFG (6 mm^3/s). The total number of contacting grains per second and the percentage of contacting grains (given in the parenthesis) are 85,848 (3.8%) in FFG and 337,568 (18%) in SRG. Of this, the total number of cutting grains per second and the percentage of cutting grains (given in the parenthesis) are 3246 (0.14%) in FFG and 33,595 (1.79%) in SRG. Even though the number of total grains passing through the grinding zone in both cases is ~2 million, the actual percentage of cutting grains is only 0.143% in FFG and 1.79% in SRG. So, an extremely small percentage of grains participate in the cutting process. Similarly, the actual percentage of contacting grains is only 3.8% in FFG and 18% in SRG. Thus most of these contacting grains do not participate in cutting but merely rub and plow into the workmaterial. The number of grains per unit area was determined by such techniques as carbon-black replica technique for the same wheel and is reported to be 295 grains/cm^2 or 1930 grains per $in.^2$ [4] while the analytical value of the apparent number of grains per cm^2, N_a, in this investigation, is found to be ~600. The replica technique is capable of counting only the larger grains and gives about half of the number of N_a. Thus, the replica technique underestimates the number of actual grains by a factor of 2. Actually, the carbon replica technique gives the number contacting points of the abrasive with the carbon soot and gives neither the actual number of the contacting grains nor the apparent number of grains per unit area.

Let us now compare the cut-off operation for two resin bonded wheels of different grain sizes, namely, 24 (Case 4) and 46 (Case 2). The mean diameters of the abrasive grains are 0.323 mm for the 46-grain size and 0.676 mm for the 24-grain size. The total number of grains in the grinding wheel passing through the cutting zone per second for the 46-grain size is 1.877×10^6 while that for the 24-grain size is nearly half (~0.858×10^6). However, the depth of wheel indentation for 46-grain size is 0.025 mm while that for the 24-grain size is 0.062 mm. The total number of contacting grains per second and the percentage of the contacting grains (given in the parenthesis) are 337,568 (18%) for the 46-grain size compared to 46,403 (10.83%) for the 24-grain size. Of this, the total number of cutting grains per second and the percentage of cutting grains given in the parenthesis are 33,600 (1.79%) for the 46-grain size while 6800 (1.6%) for the 24-grain size wheel. Even though the total number of grains passing through the cutting zone is 1.877×10^6 for the 46-grain and 0.858×10^6 for the 24-grain size, the actual percentages of cutting grains are only 1.79% for the 46-grain and 1.59% for the 24-grain size wheel. So, an extremely small percentage of grains participate in the cutting process and remove material in the form of chips. Similarly, the actual percentage of contacting grains is only 18% for the 46-grain size and 10.83% for the 24-grain size. Most of these contacting grains do not participate in cutting but merely rub and plow the workmaterial. The number of grains per unit area is 620.59 grains/cm^2 for the 46-grain size compared to 141.72 grains per cm^2 for the 24-grain size wheel. The total number of contacting grains is 111.62 grains/cm^2 for the 46-grain size compared to 15.34 grains/cm^2 for the 24-grain size wheel. The total number of actual cutting grains per unit area is 11.11 grains/cm^2 for the 46-grain size compared to 2.26 grains/cm^2 for the 24-grain size wheel.

6. Conclusions

1. In this investigation, the grinding process (both fine grinding and cut-off grinding) was considered as a stochastic process and the mechanics of the grinding process was analyzed analytically using probability statistics.
2. Various parameters of the grinding process including the number of abrasive grains in actual contact, the number of actual cutting grains per unit area under a given depth of wheel indentation, the minimum diameter of the contacting and cutting grains, and the average volume of the chip were determined analytically and compared with the experimental results reported in the literature.
3. It is found that out of a large number of grains on the surface of the wheel, only a small fraction of the grains participate in actual cutting (~0.15% in FFG with 46-grit, ~1.8% in cut-off with 46 grain, and 1.6% in cut-off with 24 grain) while a large number of contacting grains merely rub or plow (~3.62% in FFG

Table 2
Summary of grinding wheel specifications, grinding conditions, and statistical parameters in FFG and cut-off operations (Table speed: 20.32 mm/s)

#	Grinding category	Grinding wheel	Wheel speed (mm/s)	Down-feed (mm/s)	ℓ (mm)	d_{max} (mm)	d_{min} (mm)	d_{mean} (mm)	N_ℓ (grains/cm)	N_a (grains/cm^2)	N_{total} (grains/s) $\times 10^6$	Δ_{ind} (mm)	$d_{cont.min}$ (mm)	$d_{cut.min}$ (mm)	$N_{total.cont}$ (grains/s)	$N_{total.cut}$ (grains/s)	$N_{a.cont}$ (grains/cm^2)	Actual contact (%)	$N_{a.cut}$ (grains/cm^2)	Actual cut (%)	$V_{rmv.anl}$ (mm^3/s)	$V_{rmv.exp}$ (mm^3/s)
1	FFG	A46H8V	30.48		2.18	0.354	0.291	0.323	24.26	588.34	2.277	0.019	0.335	0.3441	85,848	3246	22.18	3.77	0.84	0.14	6.04	6
2	Cut-off	A46R6B	63.50	6.392	25.40	0.354	0.291	0.323	24.91	620.59	1.877	0.025	0.329	0.338	337,568	33,595	111.62	17.99	11.11	1.79	773	773
3	Cut-off	A46R6B	63.50	6.265	50.80	0.354	0.291	0.323	24.91	620.59	1.77	0.025	0.329	0.337	333,802	32,950	110.38	17.79	10.90	1.76	1516	1516
4	Cut-off	A24R6B	63.50	6.519	25.40	0.762	0.589	0.676	11.90	141.72	0.858	0.062	0.699	0.718	46,403	6839	15.34	10.83	2.26	1.60	789	789
5	Cut-off	A24R6B	63.50	6.308	50.80	0.762	0.589	0.676	11.90	141.72	0.858	0.062	0.700	0.718	45,424	6625	15.02	10.60	2.19	1.55	1526	1526

with 46-grit, ~16.2% in cut-off with 46 grain, and 9.23% in cut-off with 24 grain) and not cut at all, thus validating Hahn's rubbing grain hypothesis [9–11].

Acknowledgements

This project was initiated by a grant from the NSF US–China co-operative research project on the Thermal Aspects of Manufacturing. One of the authors (R.K.) thanks Dr. Alice Hogen of NSF for facilitating this activity and for her interest in this project. The authors are indebted to NSF for their continuing support to one of the authors (R.K.) at OSU on the various aspects of the manufacturing processes. Thanks are due, in particular, to Drs. W. DeVries, G. Hazelrigg, and D. Durham of the Division of Design, Manufacturing, and Industrial Innovation (DMII); to Dr. B. M. Kramer, of the Engineering Centers Division; and to Dr. Jorn Larsen Basse of Tribology and Surface Engineering program. One of the authors (R.K.) also thanks the A. H. Nelson, Jr. Endowed Chair in Engineering for additional financial support.

Appendix A

Table A1.

Appendix B

Table B1.

Appendix C

Table C1.

Appendix D. Example of fine grinding

The following are details of the grinding wheel specifications and grinding conditions for surface grinding [3]

Table A1
Percentage volume of bond, grain, and pores in vitrified bonded white aluminum oxide (C34) grinding wheel [31,32]

Grain size	Wheel specification	Bond (wt.%)	Bond (vol.%)	Grain (vol.%)	Pores (vol.%)
24–60	24F8-V	5	4	48	48
24–60	24H8-V	7	6	48	46
24–60	24J8-V	9	8	48	44
24–60	24L8-V	11	10	49	41
24–60	24N8-V	14	14	50	36

Grinding wheel: 32A46-H8V (alumina abrasive, 46-grit size, vitreous bond, hardness *H*, and structure 8)
Wheel speed, V_{wheel}: 30.48 m/s (6000 fpm)
Table speed, v_{table}: 20.32 mm/s (4 fpm)
Width of cut, b: 12.7 mm (0.5 in.)
Downfeed, a_0: 0.0254 mm (0.001 in.)

The local elastic deflections of the wheel under load was determined using Hertzian contact loading and found to be ~0.75 μm while the deflection of the machine tool system under load for this application was estimated to be ~1.25 μm. So, the total deflection is ~2 μm which should be subtracted from the nominal downfeed in FFG. The actual value of downfeed is, therefore, 0.0234 mm.

The nominal grain size of the grinding wheel is 46. Therefore:

The diameter of the largest abrasive grain, d_{max} = 0.354 mm
The diameter of the smallest abrasive grain, d_{min} = 0.291 mm
Mean diameter of the abrasive grain, $d_{mean} = (d_{max} + d_{min})/2 = 0.323$ mm
The range of grain size distribution (normal distribution), $\delta = d_{max} - d_{min} = 0.063$ mm, or $\delta/2 = 0.031$ mm

Number of grains per unit length, $N_\ell = \frac{10}{d_{mean}} \times$ (volumetric fraction of abrasives in wheel)$^{1/3}$
Volumetric fraction of abrasives in vitrified bonded wheel: 48% (see Appendix A)

$$N_\ell = \frac{10}{0.323} \times (0.48)^{1/3} = 24.26 \text{ grains/cm}$$

Number of grains per unit area, $N_a = N_\ell^2 = 588$ grains/cm^2
Number of grains per unit volume, $N_v = N_\ell^3 = 14{,}270$ grains/cm^3
Total number of grains passing through the grinding area per second, $N_{total} = v_{wheel} \times b \times N_a = 3048 \times 1.27 \times 588 = 2.277 \times 10^6$ grains/s

The material removal rates in grinding can be obtained both analytically and experimentally. Since they should be the same, it is possible to obtain the depth of wheel indentation, Δ_{ind} for a given set of grinding conditions iteratively by equating them.

The experimental removal rate for fine grinding is given by

V_{exp} = downfeed (d) × width of cut (b) × table speed (v)
Total volumetric chip removal rate, $V_{rmv.exp} = a_0 \times b \times v_{table} = 0.0234 \times 12.7 \times 20.32 \sim 6$ mm^3/s

The analytical removal rate is obtained using Eqs.

Table B1
Structure chart for resinoid bonded grinding wheels containing 25% by weight (based on bond wt.) of cryolite ([31,32]

Structure No.	Grain (vol.%)	Bond (vol.%)												
		N 26	O 24	P 22	Q 20	R 18	S 16	T 14	U 12	V 10	W 8	X 6	Y 4	Z 2
3	58	16	18	20	22	24	26	28	30	32	34	36	38	40
4	56	18	20	22	24	26	28	30	32	34	36	38	40	42
5	54	20	22	24	26	28	30	32	34	36	38	40	42	44
6	52	22	24	26	28	30	32	34	36	38	40	42	44	46
7	50	24	26	28	30	32	34	36	38	40	42	44	46	48
8	48	26	28	30	32	34	36	38	40	42	44	46	48	50

Table C1
Probability complementary function $P(p) = 1/\sqrt{2\pi}\int_p^\infty e^{-x^2/2}dx$

p	0	1	2	3	4	5	6	7	8	9
1.0	0.1586 55	0.1562 47	0.1515 04	0.1491 69	0.1468 58	0.1445 72	0.1423 09	0.1400 70	0.1400 70	0.1378 56
1.1	0.1356 65	0.1334 99	0.1313 56	0.1292 37	0.1271 42	0.1250 71	0.1230 24	0.1210 00	0.1189 99	0.1170 22
1.2	0.1150 69	0.1131 38	0.1112 31	0.1093 48	0.1074 87	0.1056 49	0.1038 34	0.1020 41	0.1002 72	0.0985 24
1.3	0.0967 99	0.0950 97	0.0934 16	0.0917 58	0.0901 22	0.0885 07	0.0869 14	0.0853 42	0.0837 92	0.0822 63
1.4	0.0807 55	0.0792 69	0.0778 03	0.0763 57	0.0749 33	0.0735 28	0.0721 44	0.0707 80	0.0694 36	0.0681 11
1.5	0.0668 06	0.0655 07	0.0642 42	0.0629 95	0.0617 79	0.0605 70	0.0593 79	0.0582 07	0.0570 53	0.0559 17
1.6	0.0547 99	0.0536 98	0.0526 16	0.0515 50	0.0505 02	0.0494 71	0.0484 57	0.0474 59	0.0464 78	0.0455 14
1.7	0.0445 65	0.0436 33	0.0427 16	0.0418 15	0.0409 30	0.0400 59	0.0392 04	0.0383 64	0.0375 38	0.0367 27
1.8	0.0359 31	0.0351 49	0.0343 80	0.0336 26	0.0328 85	0.0321 58	0.0314 44	0.0307 43	0.0300 55	0.0293 80
1.9	0.0287 18	0.0280 68	0.0274 31	0.0268 05	0.0261 92	0.0255 90	0.0250 00	0.0244 21	0.0238 54	0.0232 98
2.0	0.0227 53	0.0222 16	0.0216 92	0.0211 78	0.0206 75	0.0201 82	0.0196 99	0.0192 26	0.0187 63	0.0183 09
2.1	0.0178 65	0.0174 29	0.0170 03	0.0165 86	0.0161 78	0.0157 78	0.0153 87	0.0150 04	0.0146 29	0.0142 62
2.2	0.0139 04	0.0135 53	0.0132 10	0.0128 74	0.0125 46	0.0122 25	0.0119 11	0.0116 04	0.0113 04	0.0110 11
2.3	0.0107 24	0.0104 45	0.0101 71	0.0099 03	0.0096 42	0.0093 87	0.0091 38	0.0088 94	0.0086 57	0.0084 25
2.4	0.0081 98	0.0079 77	0.0077 61	0.0075 50	0.0073 44	0.0071 43	0.0069 47	0.0067 56	0.0065 70	0.0063 88
2.5	0.0062 10	0.0060 37	0.0058 68	0.0057 04	0.0055 43	0.0053 87	0.0052 34	0.0050 85	0.0049 41	0.0047 99
2.6	0.0046 62	0.0045 28	0.0043 97	0.0042 70	0.0041 46	0.0040 25	0.0039 08	0.0037 93	0.0036 82	0.0035 73
2.7	0.0034 68	0.0033 65	0.0032 65	0.0031 67	0.0030 73	0.0029 80	0.0028 91	0.0028 03	0.0027 18	0.0026 36
2.8	0.0025 56	0.0024 78	0.0024 02	0.0023 28	0.0022 56	0.0021 87	0.0021 19	0.0020 53	0.0019 89	0.0019 27
2.9	0.0018 66	0.0018 08	0.0017 51	0.0016 95	0.0016 42	0.0015 89	0.0015 39	0.0014 90	0.0014 42	0.0013 95
3.0	0.0013 50	0.0013 07	0.0012 64	0.0012 23	0.0011 83	0.0011 45	0.0011 07	0.0010 71	0.0010 35	0.0010 01
3.1	0.0009 68	0.0009 36	0.0009 05	0.0008 75	0.0008 45	0.0008 17	0.0007 89	0.0007 63	0.0007 37	0.0007 12
3.2	0.0006 88	0.0006 64	0.0006 41	0.0006 19	0.0005 98	0.0005 77	0.0005 58	0.0005 38	0.0005 19	0.0005 01
3.3	0.0004 84	0.0004 67	0.0004 50	0.0004 35	0.0004 19	0.0004 04	0.0003 90	0.0003 76	0.0003 63	0.0003 50
3.4	0.0003 37	0.0003 25	0.0003 13	0.0003 02	0.0002 91	0.0002 81	0.0002 70	0.0002 61	0.0002 51	0.0002 42
3.5	0.0002 33	0.0002 24	0.0002 16	0.0002 08	0.0002 00	0.0001 93	0.0001 86	0.0001 79	0.0001 72	0.0001 66
3.6	0.0001 59	0.0001 53	0.0001 48	0.0001 42	0.0001 37	0.0001 31	0.0001 26	0.0001 22	0.0001 17	0.0001 12
3.7	0.0001 08	0.0001 04	0.0001 00	0.0000 96	0.0000 92	0.0000 89	0.0000 85	0.0000 82	0.0000 79	0.0000 76
3.8	0.0000 73	0.0000 70	0.0000 67	0.0000 64	0.0000 62	0.0000 59	0.0000 57	0.0000 55	0.0000 52	0.0000 50
3.9	0.0000 48	0.0000 46	0.0000 444	0.0000 426	0.0000 409	0.0000 393	0.0000 376	0.0000 361	0.0000 346	0.0000 331
4.0	0.0000 318	0.0000 305	0.0000 292	0.0000 280	0.0000 269	0.0000 257	0.0000 247	0.0000 236	0.0000 226	0.0000 217
4.1	0.0000 207	0.0000 199	0.0000 191	0.0000 182	0.0000 175	0.0000 167	0.0000 160	0.0000 153	0.0000 147	0.0000 141
4.2	0.0000 134	0.0000 129	0.0000 123	0.0000 117	0.0000 112	0.0000 108	0.0000 103	0.0000 098	0.0000 094	0.0000 090
4.3	0.0000 086	0.0000 082	0.0000 079	0.0000 075	0.0000 072	0.0000 069	0.0000 066	0.0000 063	0.0000 060	0.0000 057
4.4	0.0000 055	0	0	0	0	0	0	0	0	0

(17a), (18) and (21). Initially, some value of wheel indentation, Δ_{ind} is assumed, which is generally ~25% of δ, where $\delta = d_{max} - d_{min}$. If the analytical value is less than the experimental value, then the initial assumed value of Δ_{ind} is less and vice versa. A new value of Δ_{ind} is considered accordingly and the process is repeated iteratively till the analytical value is the same as the experimental value. The final value of Δ_{ind} is the actual depth of the wheel indentation under the given conditions of grinding.

In the following, an initial value of Δ_{ind} = 0.018 mm was considered. Following the procedure outlined above, we get the analytical material removal rate, $V_{rmv.anl}$ of 4.451 mm^3/s. Since, the experimental material removal rate, $V_{rmv.exp}$ (6.04 mm^3/s) is higher than the analytical value. This means the initial Δ_{ind} should be higher. A new value of Δ_{ind} = 0.019 was considered and the material removal rate calculated. This has resulted in the analytical material removal rate, $V_{rmv.anl}$ of 7.22 mm^3/s, which is higher than the experimental value indicating that the assumed Δ_{ind} is too high. So, the value of Δ_{ind}, should be between 0.018 and 0.0189. Therefore, a new value of Δ_{ind} of 0.0187 is considered. Using Eqs. (17a), (18) and (21), the chip volume rate generated by the actual cutting grains, $V_{rmv.anl}$ = 6.039 mm^3/s is close to the experimental value. This means the final value of Δ_{ind} is correct. Based on that the following calculations are performed.

Refer to Fig. 5, the diameter of the smallest contacting grain,

$$d_{cont.min} = d_{max} - \Delta_{ind} = 0.354 - 0.019 = 0.336 \text{ mm.}$$

Using Eq. (10), the diameter of the smallest cutting grain,

$$d_{cut.min} = \frac{d_{cont.min}}{0.975} = \frac{0.335}{0.975} = 0.344 \text{ mm}$$

Refer to Fig. 5, the corresponding values of x_1, x_2, p_1, and p_2 are:

$$x_1 = \frac{\delta}{2} - \Delta_{ind} = 0.0314 - 0.0187 = 0.013 \text{ mm}$$

$$x_2 = x_1 + (\text{minimum cutting depth}) = x_1 + (0.025 \times d_{cut.min}) = 0.0127 + (0.025 \times 0.344) = 0.0213 \text{ mm}$$

The relevant arguments of the complimentary probability function are:

$$p_1 = x_1 \times \frac{4.4}{\delta/2} = 0.0127 \times \frac{4.4}{0.0314} = 1.778$$

$$p_2 = x_2 \times \frac{4.4}{\delta/2} = 0.0213 \times \frac{4.4}{0.0314} = 2.984$$

Using Eq. (8), the values of the complimentary probability function for p_1 and p_2, respectively, (the percentages of actual contacting and actual cutting grains) can be obtained

% actual contacting grains, $P(p_1)$ = 3.77%
% actual cutting grains, $P(p_2)$ = 0.143%.

Based on the probability of actual contacting and actual cutting grains, the following parameters are calculated

The total number of actual contacting grains passing through the grinding area, $N_{total.cont} = N_{total} \times P(p_1) = 2.277 \times 10^6 \times 0.0377 = 85{,}848$ grains/s
The total number of actual cutting grains passing through the grinding area, $N_{total.cut} = N_{total} \times P(p_2) = 2.277 \times 10^6 \times 0.00143 = 3246$ grains/s
The total number of actual contacting grains per unit area, $N_{a.cont} = N_a \times P(p_1) = 588 \times 0.0377 = 22.18$ grains/cm^2
The total number of actual cutting grains per unit area, $N_{a.cut} = N_a \times P(p_2) = 588 \times 1.43 \times 10^{-3} = 0.84$ grains/cm^2.

References

[1] M.C. Shaw, Principles of Abrasive Processes, Oxford University Press, Oxford, UK, 1996.
[2] M.C. Shaw, Fundamentals of the grinding process, in: M.C. Shaw (Ed.), Proceedings of the International Grinding Conference, Carnegie Press, Pittsburgh, PA, 1972, pp. 220–258.
[3] E.R. Marshall, M.C. Shaw, Forces in dry surface grinding, Trans. ASME 74 (1952) 51–59.
[4] W.R. Backer, E.R. Marshall, M.C. Shaw, The size effect in metal cutting, Trans. ASME 74 (1952) 61–72.
[5] J.O. Outwater, M.C. Shaw, Surface temperatures in grinding, Trans. ASME 74 (1952) 73–86.
[6] G.S. Reichenbach, J.E. Mayer, S. Kalpakcioglu, M.C. Shaw, The role of chip thickness in grinding, Trans. ASME 78 (1956) 847–859.
[7] J. Mayer, M.C. Shaw, Grinding temperatures, ASLE Lubrication Eng (1957).
[8] W.R. Backer, M.E. Merchant, On the basic mechanics of the grinding process, Trans. ASME 80 (1958) 141–148.
[9] R.S. Hahn, The effect of wheel work conformity in precision grinding, Trans. ASME 77 (1955) 1325–1329.
[10] R.S. Hahn, The relation between grinding conditions and thermal damage in the workpiece, Trans. ASME 78 (1956) 807–810.
[11] R.S. Hahn, On the nature of the grinding process, in: Advances in Machine Tool Design and Research, Pergamon Press, London, UK, 1963, pp. 129–154.
[12] R. Komanduri, Some aspects of machining with negative rake angles simulating grinding, Int. J. Mach. Tool. Des. Res. 11 (1971) 223–233.
[13] S. Malkin, Grinding technology—theory and application of machining with abrasives, Ellis Harwood Ltd, West Sussex, UK, 1989.
[14] G.W. Rowe, A.G. Wetton, Theoretical considerations in the grinding of metals, J. Inst. Metals 97 (1969) 193–200.
[15] H. Opitz, W. Konig, W. Werner, Kinematics and mechanics in grinding with regard to the machining process, in: M.C. Shaw (Ed.), Proceedings of the International Grinding Conference, Carnegie Press, Pittsburgh, PA, 1972, pp. 259–282.
[16] R. Snoeys, J. Peters, A. Decneut, The significance of chip thickness in grinding, Ann. CIRP 23/2 (1974) 227–237.
[17] K. Nakayama, Grinding wheel geometry, in: M.C. Shaw (Ed.), Proceedings of the International Grinding Conference, Carnegie Press, Pittsburgh, PA, 1972, pp. 197–219.
[18] W.B. Rowe, S.C.E. Black, B. Mills, M.N. Morgan, H.S. Qi, Grinding temperatures and energy partition, Proc. R. Soc. London A 453 (1997) 1083–1104.
[19] A. Lavine, Thermal aspects of grinding: the effect of heat generation at the shear planes, Ann. CIRP 40/1 (1991) 343–345.
[20] C. Guo, S. Malkin, Analysis of energy partition in grinding, Trans. ASME J. Eng. Ind. 117 (1995) 55–61.

[21] Y. Ju, T.N. Farris, S. Chandrasekar, Theoretical analysis of heat partition and temperature in grinding, Trans. ASME J. Tribol. 120 (1998) 789–794.
[22] M.C. Shaw, New developments in grinding, in: Proceedings of the International Grinding Conference, Carnegie Press, Pittsburgh, PA, 1972.
[23] M.C. Shaw, D.A. Farmer, K. Nakayama, Mechanics of the abrasive cut-off operation, Trans. ASME J. Eng. Ind. 89 (1967) 495–502.
[24] S. Eshghy, Thermal aspects of the abrasive cut-off operation, Part 1. Theoretical analysis, Trans. ASME 89 (1967) 356–360.
[25] S. Eshghy, Thermal aspects of the abrasive cut-off operation, Part 2. Partition Functions and Optimum Cutoff, Trans. ASME 89 (1967) 356–359.
[26] M.C. Shaw, The rating of cut-off wheels, Trans. ASME J. Eng. Ind. 97 (1975) 138–146.
[27] J.N. Brecker, M.C. Shaw, Measurement of the effective number of cutting points in the surface of a grinding wheel, in: Proceedings of the International Conference on Production Engineering, Japan Society of Precision Engineers, Tokyo, Japan, 1974, pp. 740–745.
[28] W.B. Rowe, M.M. Morgan, H.S. Qi, H.W. Zheng, The effect of deformation on the contact area in grinding, Annals. CIRP 42/1 (1993) 409–412.
[29] Specifications for the size of abrasive grain-grinding wheels, polishing and general industrial use, American National Standard ANSI B74.12-1976 (R1982).
[30] R. Komanduri, S. Iyengar, in: Conventional and Superabrasive Materials, Encyclopedia of Materials, Science and Technology, Elsevier Science Ltd, 2001, pp. 1629–1652.
[31] D.A. Farmer, J.N. Brecker, M.C. Shaw, Investigation of grinding fundamentals, First Annual Report, Grinding Wheel Institute, Carnegie Institute of Technology, Pittsburgh, PA, 1964, p. 3.
[32] D.A. Farmer, K. Nakayama, S. Eshghy, M.C. Shaw, Investigation of grinding fundamentals, Second Annual Report, Grinding Wheel Institute, Carnegie Institute of Technology, Pittsburgh, PA, 1965, p. 3.
[33] M.R. Spiegel, Mathematical Handbook of Formulas and Tables, McGraw Hill, New York, NY, 1999.
[34] R.H. Brown, K. Saito, M.C. Shaw, Local elastic deflections in grinding, Ann. CIRP 19 (1971) 105–113.
[35] H. Krug, G. Honcia, Die Elastiche Verformung bei Schleifwekzeugen, Werstattstech 54 (1964) 53.